

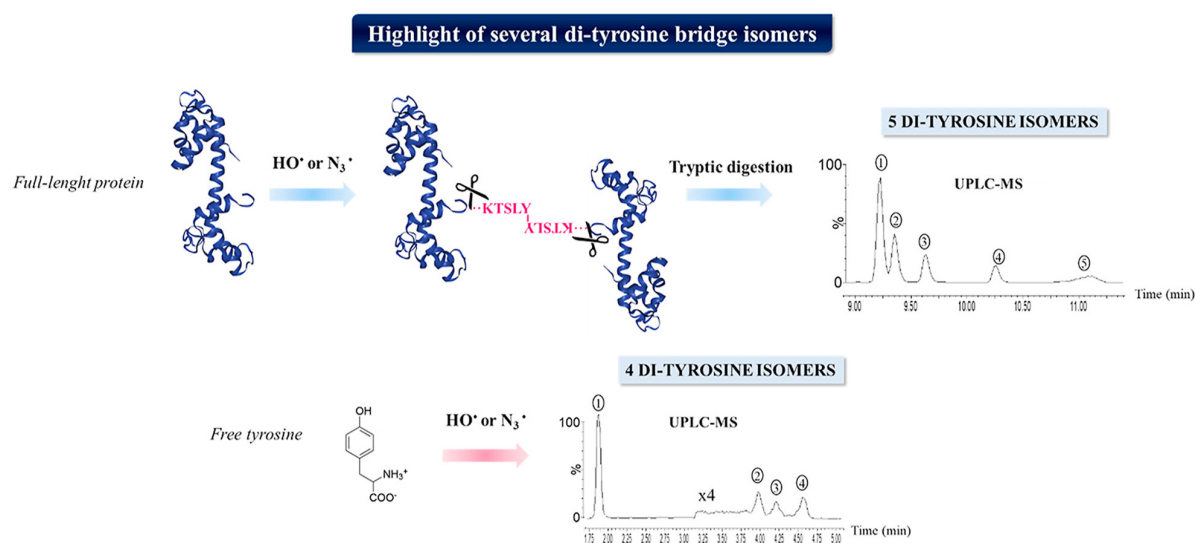
Année de publication : 2021

Anouchka Gatin, Isabelle Billault, Patricia Duchambon, Guillaume Van der Rest, Cécile Sicard-Roselli (2022 Jan 3)

### Oxidative radicals ( $\text{HO}^\bullet$ or $\text{N}_3^\bullet$ ) induce several di-tyrosine bridge isomers at the protein scale.

 Free radical biology & medicine : 162 : 461-470 : DOI : [10.1016/j.freeradbiomed.2020.10.324](https://doi.org/10.1016/j.freeradbiomed.2020.10.324)

#### Résumé



Among protein oxidative damages, di-tyrosine bridges formation has been evidenced in many neuropathological diseases. Combining oxidative radical production by gamma radiolysis with very performant chromatographic separation coupled to mass spectrometry detection, we brought into light new insights of tyrosine dimerization. Hydroxyl and azide radical tyrosine oxidation leading to di-tyrosine bridges formation was studied for different biological compounds: a full-length protein ( $\Delta 25$ -centrin 2), a five amino acid peptide (KTSLY) and free tyrosine. We highlighted that both radicals generate high proportion of dimers even for low doses. Surprisingly, no less than five different di-tyrosine isomers were evidenced for the protein and the peptide. For tyrosine alone, at least four distinct dimers were evidenced. These results raise some questions about their respective role in vivo and hence their relative toxicity. Also, as di-tyrosine is often used as a biomarker, a better knowledge of the type of dimer detected in vivo is now required.

Didier Surdez, Sakina Zaidi, Sandrine Grossetête, Karine Laud-Duval, Anna Sole Ferre, Lieke Mous, Thomas Vourc'h, Franck Tirode, Gaëlle Pierron, Virginie Raynal, Sylvain Baulande, Erika Brunet, Véronique Hill, Olivier Delattre (2021 Apr 30)

### STAG2 mutations alter CTCF-anchored loop extrusion, reduce cis-regulatory

**interactions and EWSR1-FLI1 activity in Ewing sarcoma.**

Cancer cell : [DOI : 10.1016/j.ccell.2021.04.001](https://doi.org/10.1016/j.ccell.2021.04.001)

**Résumé**

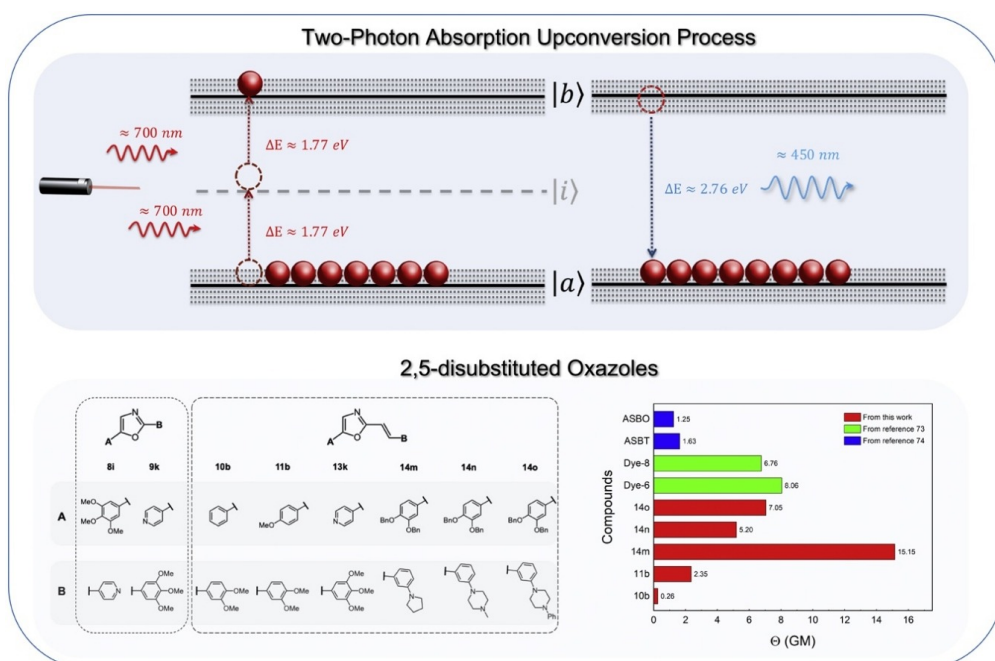
STAG2, a cohesin family gene, is among the most recurrently mutated genes in cancer. STAG2 loss of function (LOF) is associated with aggressive behavior in Ewing sarcoma, a childhood cancer driven by aberrant transcription induced by the EWSR1-FLI1 fusion oncogene. Here, using isogenic Ewing cells, we show that, while STAG2 LOF profoundly changes the transcriptome, it does not significantly impact EWSR1-FLI1, CTCF/cohesin, or acetylated H3K27 DNA binding patterns. In contrast, it strongly alters the anchored dynamic loop extrusion process at boundary CTCF sites and dramatically decreases promoter-enhancer interactions, particularly affecting the expression of genes regulated by EWSR1-FLI1 at GGAA microsatellite neo-enhancers. Down-modulation of cis-mediated EWSR1-FLI1 activity, observed in STAG2-LOF conditions, is associated with enhanced migration and invasion properties of Ewing cells previously observed in EWSR1-FLI1 cells. Our study illuminates a process whereby STAG2-LOF fine-tunes the activity of an oncogenic transcription factor through altered CTCF-anchored loop extrusion and cis-mediated enhancer mechanisms.

Abegão L.M., Santos F.A., Piguel S., Rodrigues J.J., Mendonça C.R., De Boni L. (2021 Apr 15)

**The ability of 2,5-disubstituted oxazole dyes derivatives to generate two-photon upconversion photoluminescence and its brightness evaluation**

*Journal of Photochemistry and Photobiology A: Chemistry* : 411 : 113214 : [DOI : 10.1016/j.jphotochem.2021.113214](https://doi.org/10.1016/j.jphotochem.2021.113214)

**Résumé**



The

brightness study of emissive compounds is one of the fundamental spectroscopic characterizations. In this work, we assessed the brightness values of eight 2,5-disubstituted oxazole dyes derivatives by combining linear and nonlinear spectroscopic parameters. The range of the brightness values obtained is from 0.26 GM to 15.15 GM. The highest value belongs to compound 14 m, which, compared to previously investigated compounds of similar  $\pi$ -conjugation length, is at least two times higher. Brightness values were determined in the spectral region between 700 nm–720 nm, revealing this class of dyes' potential to be used as photoluminescence bioprobes excited by two-photons.

Ophélie Lautier, Arianna Penzo, Jérôme O Rouvière, Guillaume Chevreux, Louis Collet, Isabelle Loïodice, Angela Taddei, Frédéric Devaux, Martine A Collart, Benoit Palancade (2021 Apr 10)

### Co-translational assembly and localized translation of nucleoporins in nuclear pore complex biogenesis.

*Molecular cell* : [DOI : S1097-2765\(21\)00225-2](https://doi.org/10.1016/j.molcel.2021.04.010)

#### Résumé

mRNA translation is coupled to multiprotein complex assembly in the cytoplasm or to protein delivery into intracellular compartments. Here, by combining systematic RNA immunoprecipitation and single-molecule RNA imaging in yeast, we have provided a complete depiction of the co-translational events involved in the biogenesis of a large multiprotein assembly, the nuclear pore complex (NPC). We report that binary interactions between NPC subunits can be established during translation, in the cytoplasm. Strikingly, the nucleoporins Nup1/Nup2, together with a number of nuclear proteins, are instead translated at nuclear pores, through a mechanism involving interactions between their nascent N-termini and nuclear transport receptors. Uncoupling this co-translational recruitment further

triggers the formation of cytoplasmic foci of unassembled polypeptides. Altogether, our data reveal that distinct, spatially segregated modes of co-translational interactions foster the ordered assembly of NPC subunits and that localized translation can ensure the proper delivery of proteins to the pore and the nucleus.

Tsai Feng-Ching, Simunovic Mijo, Sorre Benoit , Bertin Aurélie, Manzi John, Callan-Jones Andrew, Bassereau Patricia (2021 Apr 6)

### **Comparing physical mechanisms for membrane curvature-driven sorting of BAR-domain proteins**

*Soft Matter* : [DOI : 10.1039/D0SM01573C](https://doi.org/10.1039/D0SM01573C)

#### **Résumé**

Protein enrichment at specific membrane locations in cells is crucial for many cellular functions. It is well-recognized that the ability of some proteins to sense membrane curvature contributes partly to their enrichment in highly curved cellular membranes. In the past, different theoretical models have been developed to reveal the physical mechanisms underlying curvature-driven protein sorting. This review aims to provide a detailed discussion of the two continuous models that are based on the Helfrich elasticity energy, (1) the spontaneous curvature model and (2) the curvature mismatch model. These two models are commonly applied to describe experimental observations of protein sorting. We discuss how they can be used to explain the curvature-induced sorting data of two BAR proteins, amphiphysin and centaurin. We further discuss how membrane rigidity, and consequently the membrane curvature generated by BAR proteins, could influence protein organization on the curved membranes. Finally, we address future directions in extending these models to describe some cellular phenomena involving protein sorting.

Heltberg Mathias, Miné-Hattab Judith, Taddei Angela , Walczak Aleksandra M. , Mora Thierry (2021 Apr 2)

### **Physical observables to determine the nature of membrane-less cellular sub-compartments**

*preprint* . : [DOI : 10.1101/2021.04.01.438041](https://doi.org/10.1101/2021.04.01.438041)

#### **Résumé**

## **Abstract**

The spatial organization of complex biochemical reactions is essential for the regulation of cellular processes. Membrane-less structures called foci containing high concentrations of specific proteins have been reported in a variety of contexts, but the mechanism of their formation is not fully understood. Several competing mechanisms exist that are difficult to distinguish empirically, including liquid-liquid phase separation, and the trapping of

molecules by multiple binding sites. Here we propose a theoretical framework and outline observables to differentiate between these scenarios from single molecule tracking experiments. In the binding site model, we derive relations between the distribution of proteins, their diffusion properties, and their radial displacement. We predict that protein search times can be reduced for targets inside a liquid droplet, but not in an aggregate of slowly moving binding sites. These results are applicable to future experiments and suggest different biological roles for liquid droplet and binding site foci.

Romain-David Seban, Roman Rouzier, Aurelien Latouche, Nicolas Deleval, Jean-Marc Guinebretiere, Irene Buvat, Francois-Clement Bidard, Laurence Champion (2021 Mar 28)

**Total metabolic tumor volume and spleen metabolism on baseline [18F]-FDG PET/CT as independent prognostic biomarkers of recurrence in resected breast cancer.**

*European journal of nuclear medicine and molecular imaging* : DOI : [10.1007/s00259-021-05322-2](https://doi.org/10.1007/s00259-021-05322-2)

### Résumé

We evaluated whether biomarkers on baseline [F]-FDG PET/CT are associated with recurrence after surgery in patients with invasive breast cancer of no special type (NST).

Daniel Jeffery, Alberto Gatto, Katrina Podsypanina, Charlene Renaud-Pageot, Rebeca Ponce Landete, Lorraine Bonneville, Marie Dumont, Daniele Fachinetti, Geneviève Almouzni (2021 Mar 26)

**CENP-A overexpression promotes distinct fates in human cells, depending on p53 status**

*Communications Biology* : 4 : 1-18 : DOI : [10.1038/s42003-021-01941-5](https://doi.org/10.1038/s42003-021-01941-5)

### Résumé

Julien Robert-Paganin, Xiao-Ping Xu, Mark F Swift, Daniel Auguin, James P Robblee, Hailong Lu, Patricia M Fagnant, Elena B Kremontsova, Kathleen M Trybus, Anne Houdusse, Niels Volkmann, Dorit Hanein (2021 Mar 26)

**The actomyosin interface contains an evolutionary conserved core and an ancillary interface involved in specificity.**

*Nature communications* : 1892 : DOI : [10.1038/s41467-021-22093-4](https://doi.org/10.1038/s41467-021-22093-4)

### Résumé

Plasmodium falciparum, the causative agent of malaria, moves by an atypical process called gliding motility. Actomyosin interactions are central to gliding motility. However, the details

of these interactions remained elusive until now. Here, we report an atomic structure of the divergent *Plasmodium falciparum* actomyosin system determined by electron cryomicroscopy at the end of the powerstroke (Rigor state). The structure provides insights into the detailed interactions that are required for the parasite to produce the force and motion required for infectivity. Remarkably, the footprint of the myosin motor on filamentous actin is conserved with respect to higher eukaryotes, despite important variability in the *Plasmodium falciparum* myosin and actin elements that make up the interface. Comparison with other actomyosin complexes reveals a conserved core interface common to all actomyosin complexes, with an ancillary interface involved in defining the spatial positioning of the motor on actin filaments.

Patryk Skowron, Hamza Farooq, Florence M G Cavalli, A Sorana Morrissy, Michelle Ly, Liam D Hendrikse, Evan Y Wang, Haig Djambazian, Helen Zhu, Karen L Mungall, Quang M Trinh, Tina Zheng, Shizhong Dai, Ana S Guerreiro Stucklin, Maria C Vladoiu, Vernon Fong, Borja L Holgado, Carolina Nor, Xiaochong Wu, Diala Abd-Rabbo, Pierre Bérubé, Yu Chang Wang, Betty Luu, Raul A Suarez, Avesta Rastan, Aaron H Gillmor, John J Y Lee, Xiao Yun Zhang, Craig Daniels, Peter Dirks, David Malkin, Eric Bouffet, Uri Tabori, James Loukides, François P Doz, Franck Bourdeaut, Olivier O Delattre, Julien Masliah-Planchon, Olivier Ayrault, Seung-Ki Kim, David Meyronet, Wieslawa A Grajkowska, Carlos G Carlotti, Carmen de Torres, Jaume Mora, Charles G Eberhart, Erwin G Van Meir, Toshihiro Kumabe, Pim J French, Johan M Kros, Nada Jabado, Boleslaw Lach, Ian F Pollack, Ronald L Hamilton, Amulya A Nageswara Rao, Caterina Giannini, James M Olson, László Bognár, Almos Klekner, Karel Zitterbart, Joanna J Phillips, Reid C Thompson, Michael K Cooper, Joshua B Rubin, Linda M Liau, Miklós Garami, Peter Hauser, Kay Ka Wai Li, Ho-Keung Ng, Wai Sang Poon, G Yancey Gillespie, Jennifer A Chan, Shin Jung, Roger E McLendon, Eric M Thompson, David Zagzag, Rajeev Vibhakar, Young Shin Ra, Maria Luisa Garre, Ulrich Schüller, Tomoko Shofuda, Claudia C Faria, Enrique López-Aguilar, Gelareh Zadeh, Chi-Chung Hui, Vijay Ramaswamy, Swneke D Bailey, Steven J Jones, Andrew J Mungall, Richard A Moore, John A Calarco, Lincoln D Stein, Gary D Bader, Jüri Reimand, Jiannis Ragoussis, William A Weiss, Marco A Marra, Hiromichi Suzuki, Michael D Taylor (2021 Mar 20)

### **The transcriptional landscape of Shh medulloblastoma.**

*Nature communications* : 1749 : [DOI : 10.1038/s41467-021-21883-0](https://doi.org/10.1038/s41467-021-21883-0)

### **Résumé**

Sonic hedgehog medulloblastoma encompasses a clinically and molecularly diverse group of cancers of the developing central nervous system. Here, we use unbiased sequencing of the transcriptome across a large cohort of 250 tumors to reveal differences among molecular subtypes of the disease, and demonstrate the previously unappreciated importance of non-coding RNA transcripts. We identify alterations within the cAMP dependent pathway (GNAS, PRKAR1A) which converge on GLI2 activity and show that 18% of tumors have a genetic event that directly targets the abundance and/or stability of MYCN. Furthermore, we discover an extensive network of fusions in focally amplified regions encompassing GLI2, and several

loss-of-function fusions in tumor suppressor genes PTCH1, SUFU and NCOR1. Molecular convergence on a subset of genes by nucleotide variants, copy number aberrations, and gene fusions highlight the key roles of specific pathways in the pathogenesis of Sonic hedgehog medulloblastoma and open up opportunities for therapeutic intervention.

Elisa Le Boiteux, Franck Court, Pierre-Olivier Guichet, Catherine Vours-Barrière, Isabelle Vaillant, Emmanuel Chautard, Pierre Verrelle, Bruno M Costa, Lucie Karayan-Tapon, Anne Fogli, Philippe Arnaud (2021 Mar 15)

**Widespread overexpression from the four DNA hypermethylated HOX clusters in aggressive (IDHwt) glioma is associated with H3K27me3 depletion and alternative promoter usage.**

*Molecular oncology* : Accepted article : [DOI : 10.1002/1878-0261.12944](https://doi.org/10.1002/1878-0261.12944)

### Résumé

In human, the 39 coding HOX genes and 18 referenced non-coding antisense transcripts are arranged in four genomic clusters named HOXA, B, C, and D. This highly conserved family belongs to the homeobox class of genes that encode transcription factors required for normal development. Therefore, HOX gene deregulation might contribute to the development of many cancer types. Here, we study HOX gene deregulation in adult glioma, a common type of primary brain tumor. We performed extensive molecular analysis of tumor samples, classified according to their isocitrate dehydrogenase (IDH1) gene mutation status, and of glioma stem cells. We found widespread expression of sense and antisense HOX transcripts only in aggressive (IDHwt) glioma samples, although the four HOX clusters displayed DNA hypermethylation. Integrative analysis of expression-, DNA methylation- and histone modification signatures along the clusters revealed that HOX gene upregulation relies on canonical and alternative bivalent CpG island promoters that escape hypermethylation. H3K27me3 loss at these promoters emerges as the main cause of widespread HOX gene upregulation in IDHwt glioma cell lines and tumors. Our study provides the first comprehensive description of the epigenetic changes at HOX clusters and their contribution to the transcriptional changes observed in adult glioma. It also identified putative « master » HOX proteins that might contribute to the tumorigenic potential of glioma stem cells.

Alexandre Leduc, Samia Chaouni, Frédéric Pouzoulet, Ludovic De Marzi, Frédérique Megnin-Chanet, Erwan Corre, Dinu Stefan, Jean-Louis Habrand, François Sichel, Carine Laurent (2021 Mar 13)

**Differential normal skin transcriptomic response in total body irradiated mice exposed to scattered versus scanned proton beams.**

*Scientific reports* : 11 : 5876 : [DOI : 10.1038/s41598-021-85394-0](https://doi.org/10.1038/s41598-021-85394-0)

### Résumé

Proton therapy allows to avoid excess radiation dose on normal tissues. However, there are some limitations. Indeed, passive delivery of proton beams results in an increase in the lateral dose upstream of the tumor and active scanning leads to strong differences in dose delivery. This study aims to assess possible differences in the transcriptomic response of skin in C57BL/6 mice after TBI irradiation by active or passive proton beams at the dose of 6 Gy compared to unirradiated mice. In that purpose, total RNA was extracted from skin samples 3 months after irradiation and RNA-Seq was performed. Results showed that active and passive delivery lead to completely different transcription profiles. Indeed, 140 and 167 genes were differentially expressed after active and passive scanning compared to unirradiated, respectively, with only one common gene corresponding to RIKEN cDNA 9930021J03. Moreover, protein-protein interactions performed by STRING analysis showed that 31 and 25 genes are functionally related after active and passive delivery, respectively, with no common gene between both types of proton delivery. Analysis showed that active scanning led to the regulation of genes involved in skin development which was not the case with passive delivery. Moreover, 14 ncRNA were differentially regulated after active scanning against none for passive delivery. Active scanning led to 49 potential mRNA-ncRNA pairs with one ncRNA mainly involved, Gm44383 which is a miRNA. The 43 genes potentially regulated by the miRNA Gm44393 confirmed an important role of active scanning on skin keratin pathway. Our results demonstrated that there are differences in skin gene expression still 3 months after proton irradiation versus unirradiated mouse skin. And strong differences do exist in late skin gene expression between scattered or scanned proton beams. Further investigations are strongly needed to understand this discrepancy and to improve treatments by proton therapy.

Sylvie Gory-Fauré, Rebecca Powell, Julie Jonckheere, Fabien Lanté, Eric Denarier, Leticia Peris, Chi Hung Nguyen, Alain Buisson, Laurence Lafanechère, Annie Andrieux (2021 Mar 12)

**Pyr1-Mediated Pharmacological Inhibition of LIM Kinase Restores Synaptic Plasticity and Normal Behavior in a Mouse Model of Schizophrenia.**

*Frontiers in pharmacology* : 12 : 627995 : [DOI : 10.3389/fphar.2021.627995](https://doi.org/10.3389/fphar.2021.627995)

### Résumé

The search for effective treatments for neuropsychiatric disorders is ongoing, with progress being made as brain structure and neuronal function become clearer. The central roles played by microtubules (MT) and actin in synaptic transmission and plasticity suggest that the cytoskeleton and its modulators could be relevant targets for the development of new molecules to treat psychiatric diseases. In this context, LIM Kinase - which regulates both the actin and MT cytoskeleton especially in dendritic spines, the post-synaptic compartment of the synapse - might be a good target. In this study, we analyzed the consequences of blocking LIMK1 pharmacologically using Pyr1. We investigated synaptic plasticity defects and behavioral disorders in MAP6 KO mice, an animal model useful for the study of psychiatric disorders, particularly schizophrenia. Our results show that Pyr1 can modulate MT dynamics in neurons. In MAP6 KO mice, chronic LIMK inhibition by long-term treatment with Pyr1 can restore normal dendritic spine density and also improves long-term potentiation, both of which are altered in these mice. Pyr1 treatment improved synaptic plasticity, and also reduced social withdrawal and depressive/anxiety-like behavior in MAP6 KO mice. Overall,

the results of this study validate the hypothesis that modulation of LIMK activity could represent a new therapeutic strategy for neuropsychiatric diseases.

Simona Giunta, Solène Hervé, Ryan R White, Therese Wilhelm, Marie Dumont, Andrea Scelfo, Riccardo Gamba, Cheng Kit Wong, Giulia Rancati, Agata Smogorzewska, Hironori Funabiki, Daniele Fachinetti (2021 Mar 3)

**CENP-A chromatin prevents replication stress at centromeres to avoid structural aneuploidy.**

*Proceedings of the National Academy of Sciences of the United States of America* : [DOI : e2015634118](https://doi.org/10.1073/pnas.2015634118)

**Résumé**

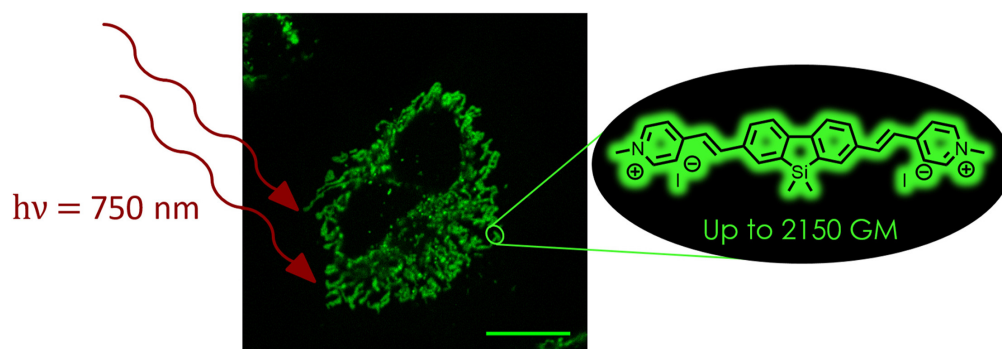
Chromosome segregation relies on centromeres, yet their repetitive DNA is often prone to aberrant rearrangements under pathological conditions. Factors that maintain centromere integrity to prevent centromere-associated chromosome translocations are unknown. Here, we demonstrate the importance of the centromere-specific histone H3 variant CENP-A in safeguarding DNA replication of alpha-satellite repeats to prevent structural aneuploidy. Rapid removal of CENP-A in S phase, but not other cell-cycle stages, caused accumulation of R loops with increased centromeric transcripts, and interfered with replication fork progression. Replication without CENP-A causes recombination at alpha-satellites in an R loop-dependent manner, unfinished replication, and anaphase bridges. In turn, chromosome breakage and translocations arise specifically at centromeric regions. Our findings provide insights into how specialized centromeric chromatin maintains the integrity of transcribed noncoding repetitive DNA during S phase.

Auvray M., Bolze F., Clavier G., Mahuteau-Betzer F. (2021 Mar 1)

**Silafluorene as a promising core for cell-permeant, highly bright and two-photon excitable fluorescent probes for live-cell imaging**

*Dyes and Pigments* : 187 : 109083 : [DOI : 10.1016/j.dyepig.2020.109083](https://doi.org/10.1016/j.dyepig.2020.109083)

**Résumé**



In this study, we report the synthesis, linear and non-linear photophysical studies and live-cell imaging of two two-photon activatable probes based on a silafluorene core: SiFluo-V and SiFluo-L. Thanks to their quadrupolar (A- $\pi$ -D- $\pi$ -A) design, these probes exhibit respectively good to impressive two-photon cross-sections (from 210 GM to 2150 GM). TD-DFT calculations support the experimental evidence that SiFluo-L displays far better two-photon absorption properties than SiFluo-V. Moreover, SiFluo-L possesses all requirements for bioimaging as it is water soluble, cell-permeant and presents a low cytotoxicity ( $IC_{80} \geq 10 \mu\text{M}$ ). It labels mitochondria in live-cell imaging at low laser power with high brightness, contrast and photostability. This study demonstrates that silafluorene is a promising core to develop new two-photon fluorophores for live-cell imaging.